Collision-induced light scattering by compressed CF_4 and CF_4-He mixtures*

D. P. Shelton, M. S. Mathur, and G. C. Tabisz
Department of Physics, University of Manitoba, Winnipeg, R3T 2N2, Canada
(Received 15 August 1974)

We have observed the collision-induced scattering from compressed CF_4 up to 70 atm and from CF_4-He mixtures at concentrations of 27%, 47%, and 48% CF_4, up to a total pressure of 155 atm. To describe the intensity distribution for pure CF_4, a single exponential function, $I = C\exp(-\omega/\omega_0)$, was fitted in the frequency range 5–20 cm^{-1}; the density dependence of ω_0 follows the scaling law derived by Fleury for rare-gas spectra. An expression involving the sum of two exponentials was fitted over a broader frequency range 5-45 cm^{-1}. It is argued that the expected intensity due to the second-order dipole-induced dipole interaction or to octupole effects is too small to account for the high-frequency tail. The shape of this tail indicates that it may arise from close encounters in which the collision time is determined principally by the intermolecular potential. The values of ω_0 determined from the spectra of the mixtures do not differ significantly from those obtained from pure CF_4. As the total pressure of the mixtures was varied, there were no sudden changes in the scattering analogous to the sharp increase of dielectric loss observed in the microwave absorption spectra and associated with the formation of dimers. In summary, the characteristics of the scattering closely resemble that from the rare gases.

INTRODUCTION

Collision-induced light scattering is essentially a translational Raman effect; the relative kinetic energy of a number of interacting molecules is altered in the scattering process. The scattering is due to a time-dependent polarizability $\Delta\alpha(t)$ induced in a cluster of interacting molecules.[1-3] The intensity distribution is then given by the Fourier transform of $\Delta\alpha(t)$,

$$I(\omega) \propto \left| \int \Delta\alpha(t) e^{i\omega t} dt \right|^2 . \quad (1)$$

Such scattering is usually observed as a broad, depolarized tail on the sharp, polarized Rayleigh line.[4] However, there have been recent reports of its occurrence in association with Raman vibrational bands.[5,6]

Since the effect exists solely because of collisions, its study, in principle, may yield information on intermolecular forces and molecular dynamics in dense media. The difficulty resides in separating the contribution in the observed scattering of the induced or cluster polarizability from that of the intermolecular potential governing the dynamics of the encounter.

Much activity has centered on the scattering from rare-gas systems.[1,3,4,7,8] The reason is simply that a free rare-gas atom has an isotropic polarizability, and consequently the scattering spectrum should be completely polarized; observed depolarized components are then entirely attributable to collision effects. Extensive studies, particularly by Fleury and his co-workers,[7,8] have been made of the gas, liquid, and solid phases of argon, xenon, and neon.

Two interaction mechanisms have been proposed to account for the induced polarizability. One is the dipole–induced-dipole (DID) interaction.[1,9,10] The external light field induces an electric dipole moment in the sample atoms. In turn, these induced dipoles interact with each other, yielding an effective pair polarizability which, to first order, is completely anisotropic and varies as r^{-3}, where r is the interatomic distance. The second mechanism is shorter in range and is caused by the overlapping of electron charge distributions during close collisions (EO).[2] In the case for helium, several calculations have been made of the dependence of the induced polarizability on interatomic distance using Hartree-Fock methods.[11,12]

Studies of the scattering from molecular systems have been concerned principally with the liquid phase.[13-15] In addition to the DID and EO mechanisms, a third is also possible. The internal degrees of freedom of the molecule can be important because a frame distortion of the molecules during collision can also give rise to an induced polarizability. Some progress had apparently been made when it was suggested[13,16] that the scattering from liquids could be accounted for by an isolated binary-collision model. The observed tail of the line profile could then be described by a compact mathematical expression in which the roles of the cluster polarizability and the intermolecular potential were clearly delineated. However, it has now been emphasized by experiment[15] and by computer calculations in molecular dynamics[17] that such a model does not satisfactorily reproduce the observed profile.

We have begun a study of collision-induced scattering from gaseous molecular systems in a re-

gime where a binary-collision model is more appropriate. In this paper, we report on the scattering from compressed CF_4, over a pressure range from 10 to 70 atm, and from CF_4-He mixtures at total pressures up to 155 atm.

CF_4 is a nonpolar spherical-top molecule of tetrahedral symmetry possessing an isotropic polarizability; it is a gas at room temperature and pressure. It has a collision-induced far-infrared absorption spectrum which is attributable to induction by the molecular octupole field.[18] In addition, in mixtures with helium, its microwave absorption spectrum displays an unusual behavior which has been associated with the formation of dimers.[19] Comparisons between the scattering, far-infrared, and microwave spectra will be useful in the analysis of the results.

EXPERIMENTAL METHOD

The apparatus used is typical of laser Raman studies. Linearly polarized light at 4880 Å from an argon-ion laser is focused by a lens (focal length 30 cm) on the sample contained within a stainless-steel pressure cell. The cell has three windows of fused silica and is capable of maintaining pressures up to 750 atm. A system of diaphragms and blackened cell walls serve to reduce stray light within the cell. The light scattered at 90° is collected by an $f/11$ system and focused on the entrance slit of a scanning double monochromator whose spectral slit width was 2 cm^{-1}. Photon-counting detection techniques are employed using a cooled RCA *C*31034 photomultiplier (PM) tube. With the discriminator levels set for an optimum signal-to-noise ratio at low light intensities, the dark count is 2–3 counts/sec. The output of the PM tube is stored in a multichannel analyzer whose channel advance is controlled by the stepping drive of the monochromator gratings. A half-wave plate and prism polarizer in the laser beam and a polarizer in the collection arm permit observations in several polarization geometries.

The CF_4 gas, purchased from the Matheson Company, Inc., had a purity of 99.7%. In order to remove a troublesome air impurity, the CF_4 sample was first frozen (the melting point is 89 K) at liquid-nitrogen temperatures in another pressure vessel which also served as a thermal compressor. As the sample was allowed to warm up to the boiling point (145 K), the oxygen and nitrogen impurities were pumped off. The degree of purification was determined by monitoring the rotational Raman scattering due to air. The helium used in the mixture was Matheson ultrahigh purity grade (99.999%).

Experiments were performed at 295 K. To remain within a pressure range where binary collisions predominate, the maximum pressure for the pure CF_4 observations was limited to 70 atm. The CF_4-He mixtures studied corresponded to 27%, 47%, and 48% CF_4 by density, with a maximum total pressure of 155 atm. The frequency range 0–75 cm^{-1} was scanned in all cases, although, at low pressures, the signal had fallen into the noise well before 75 cm^{-1}.

Amagat densities were calculated using the *P-V-T* data of MacCormack and Schneider[20] for CF_4 and Michels and Wouters[21] for He. Extrapolation of the CF_4 data for pressures above 50 atm was necessary. The partial densities of the components of the mixtures were determined following the method of Stephenson[22] and Cho.[23]

ANALYSIS OF RESULTS

Pure CF_4

Figure 1 shows the observed spectra for three densities plotted on a logarithmic intensity scale. Their general appearance is similar to spectra from the rare gases. At low density, the intensity falls off in a fashion closely exponential from the exciting frequency. As the density increases, a second slope is discernible at higher frequencies. At the highest densities studied, the identification of two distinct slopes becomes impossible, since the intensity profile curves over the entire frequency range. For gaseous argon, however, the second slope does not appear until densities of the order of the triple-point density are reached. Here, all the spectra have been taken under conditions well below the triple-point density for CF_4.

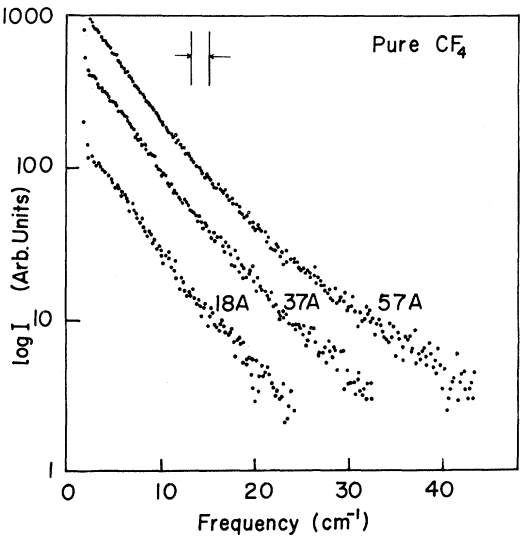

FIG. 1. Collision-induced scattering from pure CF_4 at three densities at 295 K. The vertical bars represent the spectral slit width of 2 cm^{-1}.

Because of this evolution in the shape of the spectrum, we have chosen to analyze the data in two ways: (i) by considering first a single slope and (ii) by treating two simultaneously.

Low frequencies—single exponential

Fleury and his co-workers have studied the collision-induced scattering from the rare gases (argon, neon, xenon, and krypton) over a wide range of density and temperature covering the gas, liquid, and solid phases. Assuming an exponential representation for the spectra,

$$I(\omega) = C e^{-\omega/\omega_0}, \tag{2}$$

they determine ω_0 directly from the slope of their spectra and find that it can be represented in *all* cases by an expression

$$\omega_0 = \frac{A}{2\pi c}\left(\frac{\epsilon}{M\sigma^2}\right)^{1/2}\left(\frac{kT}{\epsilon}\right)^{1/2}\left[1+\left(\frac{B\sigma^3\rho}{M}\right)^2\right], \tag{3}$$

where M is the mass, ρ is the density, and σ and ϵ are the parameters in the Lennard-Jones potential. A and B are adjustable parameters, which they found to be 3.0 ± 0.1 and 2.0 ± 0.1, respectively. For gases above the triple-point density and for solids, the relevant slope is that at high frequency. In determining that Eq. (3) holds for several different atomic systems, they have extended the corresponding-states principle to high-frequency dynamics. The corresponding-states principle usually asserts that the thermodynamic and transport coefficients, for systems with the same form of the intermolecular potential, scale directly with the parameters of that potential.

To analyze our data in a similar manner, we have fitted our spectra by an expression of the form of Eq. (2) in the frequency range 5–20 cm^{-1} using nonlinear least-squares techniques. C and ω_0 were taken as adjustable. The starting point of 5 cm^{-1} was chosen as it is sufficiently removed from the laser frequency to make errors due to stray light small. The upper limit at 20 cm^{-1} is necessary because, as will be discussed in the following section, for the higher-density spectra, the second slope becomes important at about 20 cm^{-1}. In Fig. 2, ω_0 is plotted versus density for 43 different spectra. The error bars, shown at low and high densities, represent the estimated uncertainty in the determination of ω_0 by the fitting method. There is no significant difference between the values obtained for spectra taken with various polarization geometries.

For CF_4, Eq. (3) predicts that

$$\omega_0 = 5.65[1 + (3.14\times10^{-5})\rho^2]\ cm^{-1}, \tag{4}$$

where ρ is expressed in amagat units, and $\epsilon/k = 152.5$ K and $\sigma = 4.70$ Å have been substituted.

When an expression of the form of Eq. (3) is fitted to the data in Fig. 2,

$$\omega_0 = (4.92\pm0.03)\{1+[(3.24\pm0.26)\times10^{-5}]\rho^2\}\ cm^{-1} \tag{5}$$

is found, which corresponds to $A = 2.62\pm0.02$ and $B = 2.03\pm0.05$. While these coefficients are in good agreement with the scaling law Eq. (3), the estimated standard deviation of the fit is 0.15 cm^{-1}, with discrepancies apparent, particularly at low density. Fitting a polynomial linear in density gives

$$\omega_0 = (4.63\pm0.04)\{1+[(3.32\pm0.20)\times10^{-3}]\rho\}\ cm^{-1} \tag{6}$$

with a lower estimated standard deviation of 0.11 cm^{-1}. Thus over the restricted density range of this study, a linear dependence of ω_0 on ρ gives a slightly better description of the data than does a quadratic expression.

Nevertheless, from the good agreement between Eq. (4) and Eq. (5), it may be concluded that the extended corresponding-states principle links the rare gases and CF_4 and that the Lennard-Jones potential is a good approximation to the true intermolecular potential for CF_4 for describing the dynamics effective in collision-induced scattering. Based upon their compressibility data, MacCormack and Schneider[20] also concluded that the Lennard-Jones potential is adequate in the case of

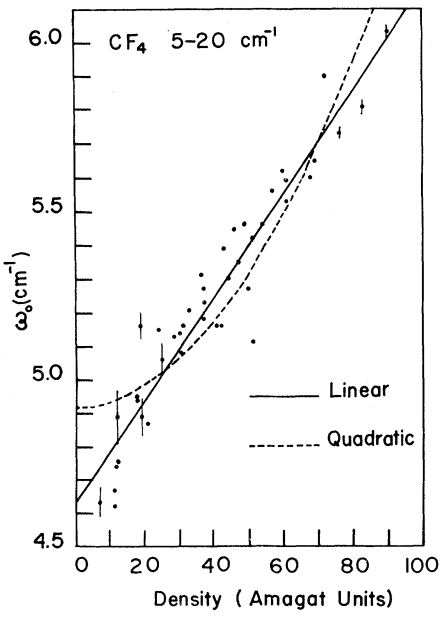

FIG. 2. Variation of ω_0 with density for pure CF_4 in the range 5–20 cm^{-1}. The dashed line represents Eq. (5) and the heavy line Eq. (6).

CF_4. Thus the intermolecular force field may be considered as central rather than localized in the outer fluorine atoms as has been suggested for the larger tetrachloride molecules, such as CCl_4.[24]

For the rare gases at low frequency and low density, it is thought that an important, but not the sole, mechanism responsible for the scattering[1,3,25] is the DID interaction. The agreement between the predictions of Eq. (3), derived for rare-gas spectra, and the present analysis indicates that, for CF_4 as well, the DID interaction predominates at low density.

High frequencies—double exponential

Since a second slope appears at high frequencies as the density increases, an expression which is the sum of two exponentials,

$$I(\omega) = Fe^{-\omega/\omega_1} + Ge^{-\omega/\omega_2}, \tag{7}$$

was also fitted to the spectra, over the range 5–45 cm^{-1}. The quality of the fits as judged from reduced χ^2 are excellent. Figure 3 shows the variation of ω_1 and ω_2 with density for spectra taken in the VH polarization geometry.[25a] While ω_1 increases steadily, ω_2 increases sharply from 30 to 50 amagat and then levels off at about 10.5 cm^{-1}. The specific values of ω_1 and ω_2 do depend upon the range chosen but their behavior with density does not change greatly. For example, the limiting value of ω_2 reaches 14.5 cm^{-1} when fits out to 70 cm^{-1} are made. Such a wide range is possible only for the highest densities. Consequently, 5–45 cm^{-1} has been selected in order to investigate changes in the profile over a reasonable density interval.

If the exponentials are extrapolated to zero frequency and integrated from zero to infinity, then the contribution of each to the total integrated intensity is obtained. The ratio of the intensities I_1/I_2 is plotted in Fig. 3. Its magnitude is about 2.5 and decreases slightly as the density increases, demonstrating that the second exponential is becoming more important.

It should be noted that when the spectra are fitted by two exponentials simultaneously, the higher-frequency component is sufficiently intense to reduce the characteristic frequency of the lower-frequency component by about 1 cm^{-1} from that obtained in the previous analysis using a single exponential only at low frequencies. The intensities of the two exponentials become equal in the region 15–20 cm^{-1}.

It is instructive to speculate on the origin of the second exponential. The factor $(1/2\pi c)(A/\sigma) \times (kT/M)^{1/2}$ in Eq. (3) is the average velocity divided by an effective range σ/A. Hence, in the binary-collision model, $(\omega_0)^{-1}$ is the duration time of the collision. Since ω_2 is greater than ω_1, the

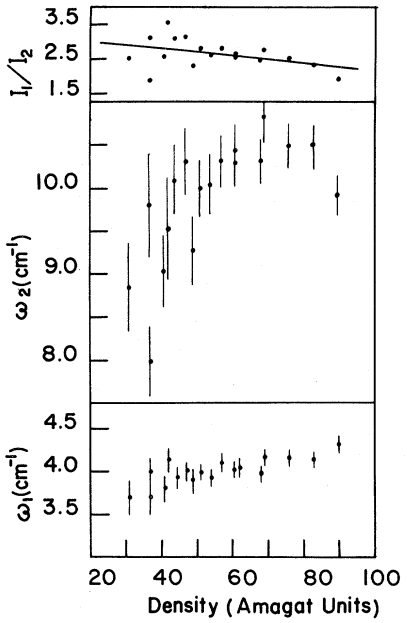

FIG. 3. Variation of ω_1, ω_2, and I_1/I_2 with density for pure CF_4 [Eq. (7)]. I_1/I_2 is the ratio of the integrated intensities of the two exponentials, $F\omega_1/G\omega_2$.

interaction giving rise to ω_2 must be of shorter duration than that producing ω_1. Several possibilities come to mind.

(i) Second-order dipole–induced dipole. The first-order dipole–induced-dipole interaction produces a pair polarizability given by

$$\Delta\alpha(r) = 6\alpha^2/r^3, \tag{8}$$

where α is the polarizability of the free atom or molecule. Classically,[9] the next higher term is $6\alpha^3/r^6$. The ratio of intensity due to first-order DID to that due to second-order DID can be estimated as

$$\frac{\text{DID1}}{\text{DID2}} = \frac{\sigma^6}{\alpha^2}\frac{H_6^{12-6}}{H_{12}^{12-6}} \approx 1640, \tag{9}$$

where

$$H_n^{12-6}/\sigma^n \propto \int r^{-n} e^{-V(r)/kT} d\tau, \tag{10}$$

and $V(r)$ is the Lennard-Jones potential. The H's involve the averaging of the intermolecular distance over the pair distribution function and have been tabulated by Buckingham and Pople.[26] The ratio 1640 is much larger than the experimentally determined 2.5, and second-order DID scattering can thus be neglected.

(ii) Octupole effects. CF_4 has a far-infrared spectrum arising from the rapidly varying dipole

moment induced during molecular collisions.[18] Because of the reasonable values of the electric octupole moment determined from this aborption intensity, the occurrence of the spectrum is attributed to induction by the octupolar fields of the colliding molecules. The octupole moment is the first nonzero multipole moment of CF_4.

Bucaro and Litovitz[13,16] studied the collision-induced scattering from liquid CCl_4 and compared it to the corresponding microwave and far-infrared absorption data of Garg *et al.*[27] In particular, they found a strong resemblance between the shapes of the absorption and the scattering profiles and concluded that the time dependence of the induced dipole moment producing the absorption spectrum is similar to the time dependence of the induced polarizability responsible for the scattering. They had determined previously that the collision-induced scattering from liquid CCl_4 was due primarily to very close encounters.

Unfortunately, such a direct comparison is not possible in the present situation. There is no reason to expect that the dipole moment and the polarizability, induced through octupole interactions, should vary similarly with time. We note, however, in passing that the far-infrared absorption profile for compressed CF_4 as determined by Rosenberg and Birnbaum[18] falls off more slowly at high frequency than does the scattering, the effective ω_0 being 27 and 11–14 cm^{-1}, respectively.

A theory describing the scattering by a pair polarizability induced through octupolar field effects has not been formulated. Rough calculations, based on the model of Buckingham and Stephen,[10] indicate that the intensity due to DID scattering would be several orders of magnitude larger than that from octupolar effects. Thus, from intensity considerations, the high-frequency scattering can not be explained by octupolar induction.

(iii) Close encounters. Bucaro and Litovitz[13] in their treatment of collision-induced scattering from liquids developed an isolated binary-collision model in which they considered the phenomenon to be entirely due to close encounters; the induction mechanisms are electron overlap and frame distortion. They calculated a collision time using a method due to Nikitin[28] and assumed a zero impact parameter and a Lennard-Jones potential. This collision time is determined solely by the dynamics and is independent of the nature of the interaction inducing $\Delta\alpha$. The characteristic frequency ω_0 is then found to be

$$(\omega_0)^{-1} = \frac{2\pi^2 c\sigma}{6}\left(\frac{M}{2kT}\right)^{1/2}\left[1-\frac{2}{\pi}\arctan\left(\frac{2\epsilon}{kT}\right)^{1/2}\right] \text{ cm}, \tag{11}$$

giving $\omega_0 = 10.3$ cm^{-1} for CF_4. Equation (11) is an approximation to an integral, performing an average over all velocities. Numerical integration yields a value about 15% higher. The agreement with our ω_2 is rather satisfactory.

A conclusion that the shape of the high frequency should be determined principally by the intermolecular potential would agree with the analytical calculations of Gersten[29] on compressed argon and with the computer experiments of Alder *et al.*[30] on argon, xenon, and neon systems. Both of these investigations used the DID interaction as the induction mechanism, thus allowing the conclusion that it is not necessary to introduce an additional interaction to account for the change of shape in the high-frequency tail.

CF_4-He mixtures

Typical spectra for the CF_4-He mixtures are presented in Fig. 4. The scattering was generally weak and varied with the square of the partial density of CF_4; only the spectra at the highest pressures showed anything other than a simple exponential tail.

Accordingly, the data were fitted to a single exponential Eq. (2) over the frequency range 5–20 cm^{-1}. The values of ω_0 are shown in Fig. 5, together with the quadratic and linear functions, Eq. (5) and Eq. (6), previously fitted to the pure CF_4 spectra. The ω_0 for the mixture spectra do not differ significantly from these curves applicable to the pure gas.

Mathur *et al.*[19] studied the nonresonant microwave absorption of CF_4-He compressed gas mixtures at 1648 MHz and found an unusual behavior.

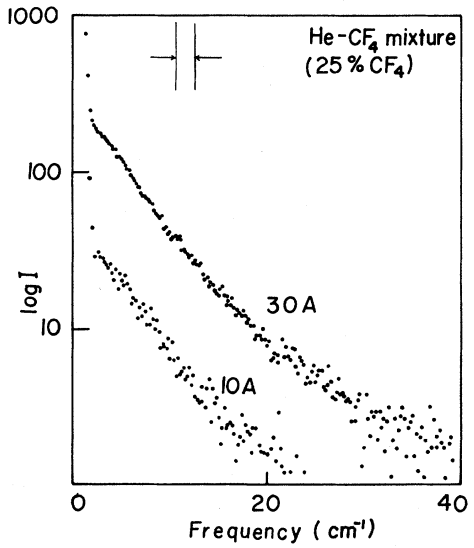

FIG. 4. Collision-induced scattering from a CF_4–He mixture (27% CF_4). The densities 30 and 10 amagat refer to the partial density of CF_4.

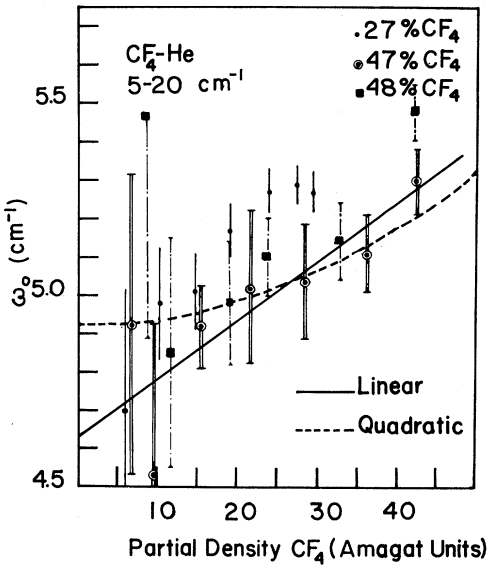

FIG. 5. Variation of ω_0 with partial density of CF_4 in the range 5–20 cm^{-1} for CF_4-He mixtures of 27%, 47%, and 48% CF_4. The dashed and heavy lines represent Eq. (5) and Eq. (6), respectively, which apply to pure CF_4.

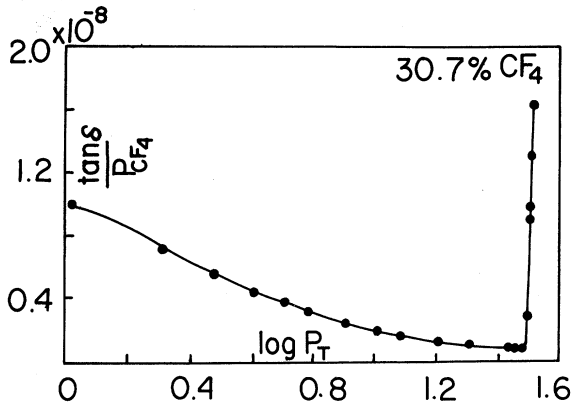

FIG. 6. Loss tangent at 1648 MHz divided by the partial pressure of CF_4 as a function of total pressure for a 30.7% mixture of CF_4 in He.

They observed a sudden onset of extreme dielectric loss at a total pressure of 33 atm for a 30.7% CF_4 mixture by volume and at a total pressure of 18.5 atm for a 55.5% mixture (Fig. 6). No such loss occurred in a 20% mixture (up to 33 atm). A phase change is not taking place as all pressures are below the critical pressure of CF_4. *P-V-T* measurements on pure CF_4 do not suggest any strong intermolecular interactions to explain this behavior.[20] They speculate that the effect is due to the formation of dimers of CF_4.

There is no indication from the collision-induced scattering to corroborate such an hypothesis. Neither the line shape (out to 20 cm^{-1}) or the intensity display any precipitous change. Our observations have been made at similar concentrations and over a wider range of total pressures. Stable dimers might add features to the spectra at low frequencies, and it is possible that the slit widths used in the present work are too broad to permit observation of them.

There is no evidence from the intensity or the line shape that CF_4-He collisions are effective in producing collision-induced scattering. Because of the small polarizability of He (2.02×10^{-25} cm^3 as compared to 1.63×10^{-24} cm^3 for argon and 3.86×10^{-24} cm^3 for CF_4), the DID interaction for He-He and CF_4-He will be very weak. However, it would be interesting to perform experiments under conditions in which the number of CF_4-He collisions per time interval is still higher than in the present study, in order to determine whether overlap-type encounters between He and CF_4 can give rise to a broad tail on the profile. It would be broad, since the low reduced mass of the collision partners will result in a short collision time.

SUMMARY

At low frequency, the slopes of the pure CF_4 spectra closely follow the scaling law developed by Fleury for rare-gas spectra. Thus scattering is chiefly due to the dipole–induced-dipole mechanism. When a wider frequency range is considered, a high-frequency tail develops with a slope smaller than that at low frequency. Intensity considerations rule out the possibility that it arises from second-order dipole–induced-dipole or octupolar effects. The magnitude of its characteristic frequency is consistent with that expected for very close collisions, where the effective collision time is determined solely by the intermolecular potential and is independent of the details of the nature of the induction mechanism. The role of CF_4-He encounters is insignificant to the scattering for the conditions of concentration and pressure studied. There were no sudden changes in intensity or line shape analogous to those observed in the microwave absorption spectrum of CF_4-He mixtures and associated with dimer formation.

In summary, the collision-induced scattering due to CF_4 at densities up to 70 amagat resembles closely the scattering from atomic rare-gas systems. No features attributable to the internal degrees of freedom of CF_4 were observed.

ACKNOWLEDGMENT

We wish to thank M. N. Neuman for his thoughtful advice concerning the computer programs.

*Supported in part by grants from the Research Corporation and from the National Research Council of Canada.

[1]M. Thibeau and B. Oksengorn, Mol. Phys. 15, 579 (1968).
[2]H. B. Levine and G. Birnbaum, Phys. Rev. Lett. 20, 439 (1968).
[3]M. Thibeau, G. C. Tabisz, B. Oksengorn, and B. Vodar, J. Quant. Spectrosc. Radiat. Transfer 10, 839 (1970).
[4]J. P. McTague and G. Birnbaum, Phys. Rev. Lett. 21, 661 (1968).
[5]W. Holzer and Y. le Duff, Phys. Rev. Lett. 32, 205 (1974).
[6]W. Holzer and R. Ouillon, Chem. Phys. Lett. 24, 589 (1974).
[7]P. A. Fleury, W. B. Daniels, and J. M. Worlock, Phys. Rev. Lett. 27, 1493 (1971).
[8]P. A. Fleury, J. M. Worlock, and H. L. Carter, Phys. Rev. Lett. 30, 591 (1973).
[9]L. Silberstein, Philos. Mag. 33, 521 (1917).
[10]A. D. Buckingham and M. J. Stephen, Trans. Faraday Soc. 53, 884 (1957).
[11]E. F. O'Brien, V. P. Gutschick, V. McKoy, and J. P. McTague, Phys. Rev. A 8, 690 (1973).
[12]A. D. Buckingham and R. S. Watts, Mol. Phys. 26, 7 (1973).
[13]J. A. Bucaro and T. A. Litovitz, J. Chem. Phys. 54, 3846 (1971).
[14]J. P. Chabrat, J. Rouch, and C. Vaucamps, Mol. Phys. 24, 897 (1972).
[15]J. H. K. Ho and G. C. Tabisz, Can. J. Phys. 51, 2025 (1973).
[16]J. A. Bucaro and T. A. Litovitz, J. Chem. Phys. 55, 3585 (1971).
[17]B. J. Berne and M. Bishop, J. Chem. Phys. 58, 2696 (1973).
[18]A. Rosenberg and G. Birnbaum, J. Chem. Phys. 48, 1396 (1968).
[19]M. S. Mathur, E. B. Bradley, and K. P. Kadaba, Mater. Sci. Eng. 1, 342 (1967).
[20]K. E. MacCormack and W. G. Schneider, J. Chem. Phys. 19, 845 (1951).
[21]A. Michels and H. Wouters, Physica 8, 923 (1941).
[22]F. C. Stephenson, Ph.D. thesis (University of Toronto, 1953) (unpublished).
[23]C. W. Cho, E. J. Allin, and H. L. Welsh, Can. J. Phys. 41, 1991 (1963).
[24]J. H. Hildebrand, J. Chem. Phys. 15, 727 (1947).
[25]H. B. Levine and G. Birnbaum, J. Chem. Phys. 55, 2914 (1971).
[25a]The incident beam is polarized in the vertical (V) direction. The direction of observation is at right angles to the direction of propagation and of polarization of the incident beam. The horizontally (H) polarized scattered component is observed; that is, it is polarized in the direction parallel to the direction of propagation of the incident beam.
[26]A. D. Buckingham and J. A. Pople, Trans. Faraday Soc. 51, 1029 (1955).
[27]S. K. Garg, J. E. Bertie, H. Kilp, and C. P. Smyth, J. Chem. Phys. 49, 2551 (1968).
[28]E. E. Nikitin, Opt. Spectrosk. 6, 91 (1959) [Opt. Spectrosc. 6, 93 (1959)].
[29]J. I. Gersten, Phys. Rev. A 4, 98 (1971).
[30]B. J. Alder, H. L. Strauss, and J. J. Weis, J. Chem. Phys. 59, 1002 (1973).